



**HAL**  
open science

## Enhanced electrochromism in short wavelengths for NiO:(Li, Mg) films in full inorganic device ITO/NiO:(Li, Mg)/Ta<sub>2</sub>O<sub>5</sub>/WO<sub>3</sub>/ITO

Dongmei Dong, Wenwen Wang, Antoine Barnabé, Lionel Presmanes, Aline Rougier, Guobo Dong, Fan Zhang, Hang Yu, Yingchun He, Xungang Diao

### ► To cite this version:

Dongmei Dong, Wenwen Wang, Antoine Barnabé, Lionel Presmanes, Aline Rougier, et al.. Enhanced electrochromism in short wavelengths for NiO:(Li, Mg) films in full inorganic device ITO/NiO:(Li, Mg)/Ta<sub>2</sub>O<sub>5</sub>/WO<sub>3</sub>/ITO. *Electrochimica Acta*, 2018, 263, pp.277-285. 10.1016/j.electacta.2018.01.049 . hal-01737285

**HAL Id: hal-01737285**

**<https://hal.science/hal-01737285>**

Submitted on 29 Oct 2019

**HAL** is a multi-disciplinary open access archive for the deposit and dissemination of scientific research documents, whether they are published or not. The documents may come from teaching and research institutions in France or abroad, or from public or private research centers.

L'archive ouverte pluridisciplinaire **HAL**, est destinée au dépôt et à la diffusion de documents scientifiques de niveau recherche, publiés ou non, émanant des établissements d'enseignement et de recherche français ou étrangers, des laboratoires publics ou privés.



## Open Archive Toulouse Archive Ouverte (OATAO)

OATAO is an open access repository that collects the work of Toulouse researchers and makes it freely available over the web where possible

This is an author's version published in: <http://oatao.univ-toulouse.fr/24519>

**Official URL:** <https://doi.org/10.1016/j.electacta.2018.01.049>

### To cite this version:

Dong, Dongmei and Wang, Wenwen and Barnabé, Antoine  and Presmanes, Lionel  and Rougier, Aline and Dong, Guobo and Zhang, Fan and Yu, Hang and He, Yingchun and Diao, Xungang *Enhanced electrochromism in short wavelengths for NiO:(Li, Mg) films in full inorganic device ITO/NiO:(Li, Mg)/Ta2O5/WO3/ITO.* (2018) *Electrochimica Acta*, 263. 277-285. ISSN 0013-4686

Any correspondence concerning this service should be sent to the repository administrator: [tech-oatao@listes-diff.inp-toulouse.fr](mailto:tech-oatao@listes-diff.inp-toulouse.fr)

# Enhanced electrochromism in short wavelengths for NiO:(Li, Mg) films in full inorganic device ITO/NiO:(Li, Mg)/Ta<sub>2</sub>O<sub>5</sub>/WO<sub>3</sub>/ITO

Dongmei Dong<sup>a</sup>, Wenwen Wang<sup>a</sup>, Antoine Barnabé<sup>b</sup>, Lionel Presmanes<sup>b</sup>,  
Aline Rougier<sup>c</sup>, Guobo Dong<sup>a</sup>, Fan Zhang<sup>a</sup>, Hang Yu<sup>a</sup>, Yingchun He<sup>a</sup>, Xungang Diao<sup>a,\*</sup>

<sup>a</sup> Electrochromic Center, School of Physics and Nuclear Energy Engineering, Beihang University, Beijing 100191, PR China

<sup>b</sup> CIRIMAT, Université de Toulouse, CNRS, INPT, UPS, Université Toulouse 3 Paul Sabatier, 118 route de Narbonne, 31062 Toulouse Cedex 9, France

<sup>c</sup> CNRS, Univ. Bordeaux, ICMCB, UPR 9048, F-33600 Pessac, France

## ARTICLE INFO

### Keywords:

Electrochromism  
Full inorganic device  
NiO:(Li, Mg) thin films

## ABSTRACT

Great interest has been drawn to the electrochromism demonstrated by inorganic materials, leading to various applications including smart windows and displays. NiO, as a cheap material, shows anodic electrochromism and is highly suitable for device applications in conjunction with WO<sub>3</sub>, but its strong optical absorbance has been largely overlooked. Herein, improved electrochromic properties in particular in short wavelengths was achieved by co doping of Mg and Li in NiO:(Li, Mg) thin films grown using RF sputtering. Secondary Ion Mass Spectroscopy technique in combination with X ray Photoelectron Spectroscopy characterization provides direct evidence of the introduction of Mg as well as Li in the film. Whatever the Li and Mg content, X Ray Diffraction and Raman spectroscopy studies only bring out the NiO face centered cubic rock salt structure. Electrochemical cycling shows pronounced anodic electrochromism for NiO:(Li, Mg) thin films. Inorganic all solid state monolithic multilayered devices are traditionally composed of a pair of electrodes with NiO and WO<sub>3</sub> separated by Li containing electrolyte such as LiTaO<sub>3</sub> or LiNbO<sub>3</sub> sputtered from expensive but low efficient ceramic targets. Based on optimal NiO:(Li, Mg) films, large switchable electrochromism both in visible (~58%) and ultraviolet band (~50%) is reconciled in electrochromic device Glass/ITO/NiO:(Li, Mg)/Ta<sub>2</sub>O<sub>5</sub>/WO<sub>3</sub>/ITO. The co doping of NiO with Mg and Li is capable of simultaneously widening the gap and avoiding the use of Li containing electrolyte, through NiO pre lithiation. We believe the new, low cost approach would provide references with respect to practical applications desired for their successful commercial mass production.

## 1. Introduction

Among inorganic electrochromic (EC) materials, NiO has been largely studied as a promising candidate to commercially substitute used IrO<sub>x</sub>. Anodic electrochromism takes place upon ions intercalation/desintercalation, and is associated with an optical transmittance modulation [1], that can be described in a band structure model, with Fermi level changes [2]. NiO is known as a good candidate for EC device [3], but a remaining issue is the residual optical absorption in the 400 < λ < 500 nm wavelength range, consequently precluding a fully transparent state [4]. Indeed, the modulation in the ultraviolet band has been rarely studied and reversely most research focus on improving EC behaviors in the

wide visible region, mainly because it is thought to be less meaningful to adjust transmittance in the known narrow wavelength range without realizing its relevance to the important color neutrality. Although the switching in short wavelength has been long time overlooked, adding proper dopants is expected to deliver enhanced bleached transparency at λ < 500 nm due to the broadened optical band gap and corresponding decreased absorbance [5]. C.G. Granqvist et al. [6] have reported that the bleached state absorbance could be significantly lowered when the additive is Mg, Al, Si, i.e., a type known to form oxides with large optical band gaps. The charge capacity will not be impaired by this doping. Similar interest in NiO thin films was reported by Chen et al. pointing out the lack of understanding for such effect [7]. They report improve transparency for Mg<sub>x</sub>Ni<sub>1-x</sub>O thin films up to x = 0.52 over a wide ultraviolet–visible spectral range. The authors found that the electronic structures are mainly a result of hybridization of Ni 3d and O 2p in the NiO<sub>6</sub> octahedra and the reduction of the

\* Corresponding author.

E-mail address: diaoxg@buaa.edu.cn (X. Diao).

Zhang Rice bound state following Mg doping.

In our work, co addition of Li and Mg is investigated for sputtered NiO thin films. More precisely, the influence of the power applied to the Li Mg alloy target, leading to possible Li Mg insertion in NiO layer, on composition, structure, morphological properties and electrochemical as well as optical behaviors, is extensively studied. The role of Mg additive in NiO is aimed to eliminate the absorption in the transparent state, and to improve the electrochromism, especially in the short wavelength range. Our current research demonstrates that enhanced bleached transparency in short wavelength region without compromising charge capacities in fact, superior to that of pure NiO can be found in optimized NiO:(Li, Mg) thin film material.

Many designs of EC devices containing gel, semi solid or polymer electrolyte in a sandwich structure have been proposed [8]. However, systems composing of solid thin films are superior to lamination structure with respect to reliability, durability and large area applications [9,10]. Therefore, it is of particular interest to search monolithic system fabrication approaches in order to achieve cost effectively and commercial displays. Great attention has been paid to the replacement of the liquid, gel, semi solid or polymer ion conductors with inorganic typical lithium salts based electrolyte (eg. LiTaO<sub>3</sub>, LiNbO<sub>3</sub>, LiPON) sputtered from low efficient, high cost ceramic targets [11,12], remaining complex technological and costing issues desired to be solved for commercial purposes. The relative shortcomings of Li containing electrolytes constitute a big obstacle towards the development of monolithic EC devices. Differently, the co doping of NiO with Mg and Li has the advantage of simultaneously widening the gap and avoiding the use of Li containing electrolyte, through NiO pre lithiation. The optimal device Glass/ITO/NiO:(Li, Mg)/Ta<sub>2</sub>O<sub>5</sub>/WO<sub>3</sub>/ITO is expected to be capable of displaying excellent EC behaviors and large switchable electrochromism in short wavelengths. Li in NiO layer is the main factor contributing to the color change. Ta<sub>2</sub>O<sub>5</sub> functions as ion conductor to make the device complete, assuring the optical modulation. This simplified, low cost and new device design is valuable for inorganic EC applications desired for commercial production and opens a different direction for achieving large, switchable electrochromism in full optical spectra.

## 2. Experimental section

**Deposition:** NiO:(Li, Mg) films were deposited by direct current (DC) magnetron co sputtering from one Ni (99.99%) metal target and one Li Mg alloy target onto bare glass, coated glass with Indium Tin Oxide (ITO) or quartz substrates (for optical band gap calculation). The Ar/O<sub>2</sub> mixture gas flow was fixed at 47/6, base pressure at 2.5 Pa, and target to substrate separation distance at 17 cm.

Li Mg content was modulated by applying various powers, from 0 to 80 W, to Li Mg alloy target while it was kept constant to 250 W for Ni target. The thickness of the films was determined by Alpha step apparatus (Dektak6M). As a result of much higher growth rate for NiO films ( $\approx 20$  nm/min) as compared to Li<sub>x</sub>Mg<sub>y</sub>O ( $\approx 2$  nm/min) independently of the Li Mg alloy target power, co sputtered films exhibit the same average thickness of 450 nm ( $440 \pm 20$ ,  $435 \pm 20$ ,  $420 \pm 20$  and  $465 \pm 20$  nm for 0, 10, 25 and 80 W, respectively). The corresponding samples from different Li Mg powers are further called NiO 0 W, NiO:(Li, Mg) 10 W, NiO:(Li, Mg) 25 W and NiO:(Li, Mg) 80 W.

The EC device Glass/ITO/NiO:(Li, Mg)/Ta<sub>2</sub>O<sub>5</sub>/WO<sub>3</sub>/ITO was deposited layer by layer. The parameters used for the other layers of the full device are summarized in Table 1.

**Characterization:** Elemental compositions were determined by Secondary Ion Mass Spectroscopy (SIMS) and X ray Photoelectron Spectroscopy (XPS) using a Cameca IMS4FE6 and Thermofisher

ESCALAB 250Xi apparatus, respectively. X Ray Diffraction (XRD) and Raman spectroscopy were used for the structural characterizations. XRD patterns were recorded with a Rigaku D/Max 2200 diffractometer using Cu K<sub>α</sub> source ( $\lambda = 1.5405 \text{ \AA}$ ). Raman spectra were collected under ambient conditions using Horiba Jobin Yvon LabRAM HR 800 spectrometer equipped with a fiber coupled 532 nm laser. Spectra acquisition was carried out for 300 s using a  $\times 100$  objective lens and 600 gr/mm grating. During the measurement, the resulting laser power at the surface of the sample was adjusted to 1.7 mW. The surface topography of the films was observed by a Nanosurf Easyscan 2 Atomic Force Microscope (AFM).

**Electrochemical and optical measurements:** Cyclic voltammetry (CVs) measurements were carried out in conventional three electrode cell configuration on a Princeton VersaSTAT 4 electrochemical workstation. Ag/AgCl was used as reference electrode and Pt as counter electrode. The UV VIS optical transmittance, absorbance and reflectance of the films was measured on a Jasco V 570 UV/VIS/NIR spectrophotometer.

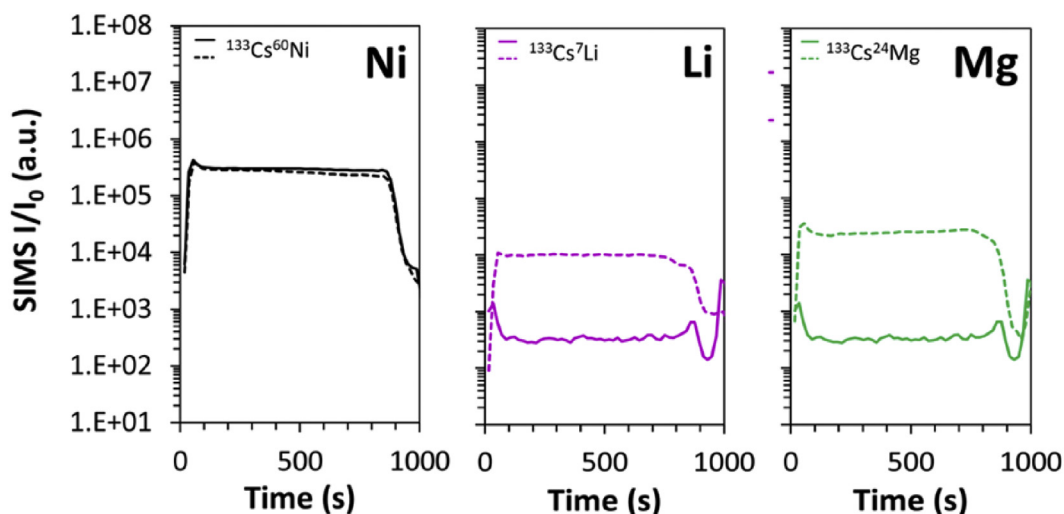
## 3. Results and discussion

### 3.1. Composition and valence states

To prove the successful introduction of Li and Mg, the compositional analysis was conducted by SIMS and XPS characterizations. SIMS profile shown in Fig. 1 exhibits the composition comparison of pure NiO and NiO:(Li, Mg) 25 W films. In panel (a), the Ni concentration in both films remains exactly at the same level from the top surface ( $t = 0$  s) to the substrate interface that appears at around 900 s. In this region, namely, NiO layer, the Ni element is uniformly distributed. This uniform elemental distribution along depth is also found in the profiles of Li and Mg as depicted in panels (b) and (c). In order to eradicate any discrepancies and make the SIMS analysis more precise, the Cs<sup>+</sup> cluster signal (<sup>133</sup>Cs<sup>7</sup>Li and <sup>133</sup>Cs<sup>24</sup>Mg) was also applied for detection in complement to <sup>7</sup>Li and <sup>24</sup>Mg. Both of the different mass signals of <sup>133</sup>Cs<sup>7</sup>Li, and <sup>133</sup>Cs<sup>24</sup>Mg show a significant increase and homogeneous distribution in the NiO:(Li, Mg) 25 W film compare to the pure NiO film corresponding to a much higher degree of both Li and Mg concentrations. However, even if the SIMS results are a powerful evidence of the existence of the two elements within NiO films, quantification is very challenging because of matrix and charging effects and finally is only possible with the use of standards (in order to define the Relative Sensitivity Factor RSF), which provides the conversion from measured SIMS intensities (second ion yield signal) to impurity density (atoms/cm<sup>3</sup>) or concentration (ppm, ppb, %, ...) and is not always proportional to their real concentration. Even though SIMS is generally considered to be a qualitative technique due to the large variation in ionization probabilities among different materials, quantification of Ni and Li in the films cannot be realized here because of the large RSF difference of the two different elements due to the matrix and charging effects. For instance, one element in a proper amount could then appear in various SIMS intensities in different matrix (see for instance Si in Si, SiC, Si<sub>3</sub>N<sub>4</sub> and SiO<sub>2</sub> matrix in B. Kasel et al. [13].) and two different elements could be detected with SIMS intensities not proportional to their real concentration. In our case, i.e. in Fig. 1b, only the SIMS intensities are reported. The impurity density is not provided. The relative intensities of Li in NiO and NiO(Li, Mg) materials can be compared whereas the matrix and charging effects are supposed to be identical. Fig. 1a clearly indicates that Ni SIMS intensities are identical. Fig. 1b and c shows significant increase and homogeneous Li and Mg distribution confirming the presence of both Li and Mg in the NiO:(Li, Mg) 25 W film as compared to NiO film. It is worth noting that two elements (Ni, Li) could be detected with variable SIMS intensities not always

**Table 1**Deposition parameters for EC device: Glass/ITO/NiO:(Li, Mg)/Ta<sub>2</sub>O<sub>5</sub>/WO<sub>3</sub>/ITO.

Target	Power source	Pressure (Pa)	Ar:O <sub>2</sub>	Power (W)	Time (min)
Ni	DC	2.5	47:6	250	20
Li-Mg alloy	Pulse	2.5	47:6	0; 10; 25; 80	20
Ta	DC	1.2	9.5:9.5	290	40
W	DC	2.2	27:9	250	18
ITO	DC	0.3	49.6:0.4	250	18

**Fig. 1.** SIMS depth profiling of elements Ni, Mg and Li in NiO (solid line) and NiO:(Li, Mg) 25 W (dashed line). Revised version.

proportional to their real concentration due to matrix effects, so they cannot be compared. But for one element Ni (the first panel of Fig. 1), it can be compared in an equivalent matrix. For one element Li or Mg (the second or third panel of Fig. 1), it can also be compared.

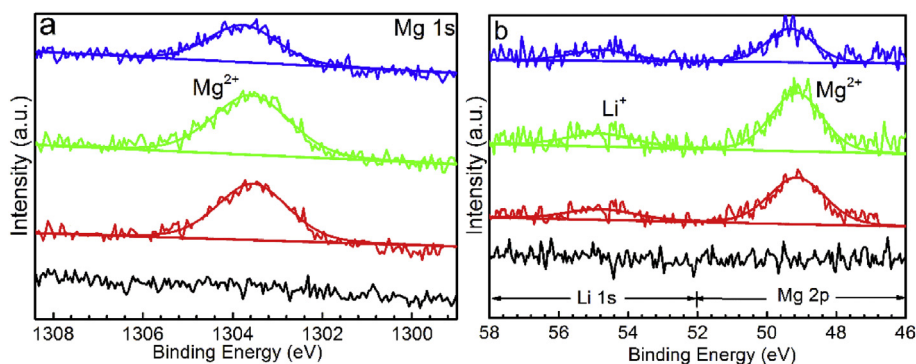
XPS typical spectrum of NiO:(Li, Mg) thin films in panels (a) and (b) of Fig. 2 directly demonstrate that the NiO:(Li, Mg) films contain the elements Mg as well as Li in agreement with the previous SIMS analysis. In Fig. 2a the scans of all NiO:(Li, Mg) thin films exhibit a broad and asymmetric peak at 1303.6 eV, corresponding to the Mg 1s peak of Mg<sup>2+</sup> [14–16]. The Mg presence is also confirmed by the Mg 2p peak at around 49 eV visible on Fig. 2b. The Li presence is highlighted in Fig. 2b by the Li 1s peak at around 55 eV. Based on the ratio of cations to anions specified by the chemical formula and atomic percentage (Table 2), NiO:(Li, Mg) film compositions were

**Table 2**

Composition of NiO:(Li, Mg) thin films deduced from XPS measurements.

Power of Li-Mg alloy	0	10	25	80
Atomic Ni (%)	44.7	41.3	38.9	38.3
Atomic O (%)	55.3	53.9	53.7	55.9
Atomic Mg (%)	0	1.5	2.6	1.8
Atomic Li (%)	0	3.3	4.8	4.0

estimated as follows: Ni<sub>0.43</sub>Ni<sub>0.38</sub>O<sup>2-</sup>, Ni<sub>0.43</sub>Ni<sub>0.34</sub>Mg<sub>0.03</sub>Li<sub>0.06</sub>O<sup>2-</sup>, Ni<sub>0.35</sub>Ni<sub>0.37</sub>Mg<sub>0.05</sub>Li<sub>0.09</sub>O<sup>2-</sup>, and Ni<sub>0.20</sub>Ni<sub>0.49</sub>Mg<sub>0.03</sub>Li<sub>0.07</sub>O<sup>2-</sup> corresponding to Li Mg power 0 W, 10 W, 25 W and 80 W, respectively. One can note that there is a high degree of Ni<sup>3+</sup> in all the films including the pure NiO. It can be estimated approximately that Li and Mg are incorporated into the compounds up to 5% atomic ratio.

**Fig. 2.** XPS of Mg 1s (a), Mg 2p and Li 1s (b) core level peaks for pure NiO (black line) and NiO:(Li, Mg) 10 W, 25 W and 80 W (red, green and blue curves) films. (For interpretation of the references to color in this figure legend, the reader is referred to the Web version of this article.)

And the amount of Li and Mg in the nanocomposite is relative stable fluctuating within 0.03, while the concentration fluctuation of  $\text{Ni}^{2+}$  is up to 0.23.

### 3.2. Structure and morphology analysis

The XRD patterns of pure NiO and NiO:(Li, Mg) thin films are shown in Fig. 3. All XRD patterns exhibit characteristic Bragg's peak of the NiO cubic structure with a (111) preferred orientation. No traces of impurities such as MgO and/or  $\text{Li}_2\text{O}$  could be detected, suggesting that Mg and Li addition takes place within NiO structure. No obvious diffraction broadening is observed, indicating that the crystallinity remains, in good agreement with a stable crystal size value, calculated using the Debye Scherrer formula, in between 8 and 10 nm whatever the film composition. The evolution of the lattice constants based on Bragg's law shows an increase from 4.20 to 4.236 Å for NiO and NiO:(Li, Mg) 80 W, respectively. Such increase is correlated with an expansion of the unit cell volume [17] from 73.9 up to 76.0 Å<sup>3</sup>. The lattice constant evolution results from a combination of various phenomena. On a steric point of view, the additions of  $\text{Li}^+$  (0.76 Å) and  $\text{Mg}^{2+}$  (0.72 Å) ions larger than  $\text{Ni}^{2+}$  (0.69 Å) [18], well agree with an increase in the lattice constant.

The Raman spectra of pure NiO and NiO:(Li, Mg) (Fig. 4) present the characteristic of NiO Raman peaks as for instance the first order Transverse Optical (TO) and Longitudinal Optical (LO) phonons modes located at 380 and 520  $\text{cm}^{-1}$ , respectively. As the shift of the LO peaks towards high wavenumbers could be correlated to the  $\text{Ni}^{3+}$  content in the NiO phase [19], the fact that both films exhibit LO peaks significantly above 500  $\text{cm}^{-1}$  is in good agreement with the  $\text{Ni}^{2+}/\text{Ni}^{3+}$  ratio previously determined by XPS. After the Li/Mg addition into NiO, an extra active band appears around 1600  $\text{cm}^{-1}$ . Based on repeated measurements with exactly the same parameters in different zones in both pure and doped NiO, it is confirmed that the extra peak at 1600  $\text{cm}^{-1}$  arises from the additional elements. This extra peak cannot be attributed to pure MgO [20] and/or  $\text{Li}_2\text{O}$  or  $\text{LiNiO}_2$  [21,22] and then could be attributed to the specific Raman signature of the NiO Li, Mg co doping. The influence of the Li/Mg addition on the structure has not been fully understood. It is reported that presence of more Raman active

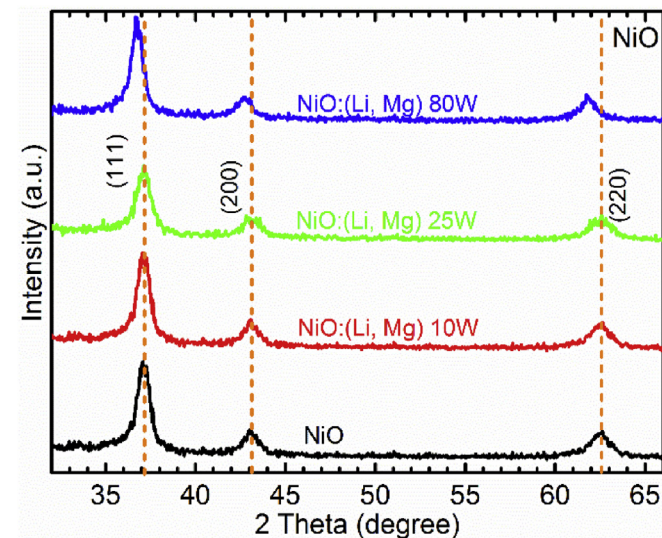


Fig. 3. XRD pattern for pure NiO (black line) and NiO:(Li, Mg) 10 W, 25 W and 80 W (red, green and blue curves) films. (For interpretation of the references to color in this figure legend, the reader is referred to the Web version of this article.)

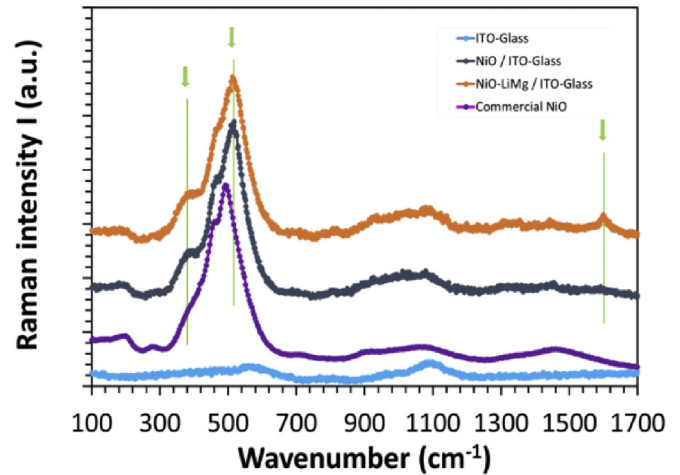


Fig. 4. Raman spectra of pure NiO and NiO:(Li, Mg) 25 W films with single ITO-glass and commercial NiO powder as reference.

bands is a sign of a distorted structure [23]. The distortion probably arises from the doping effect of guest ions. Introduction of  $\text{Li}^+$  and  $\text{Mg}^{2+}$  ions in replacement of  $\text{Ni}^{2+}$  and  $\text{Ni}^{3+}$  will globally create oxygen ion vacancies. This changes the local symmetry which induces the Li O or Mg O symmetric stretching vibrations at higher frequency region ( $>600 \text{ cm}^{-1}$ ).

The film morphologies were determined by AFM technique over an area of  $1 \times 1 \mu\text{m}^2$ . The right length scale in Fig. 5 is 1  $\mu\text{m}$ . Panel (a) shows that the pure NiO film has a distinct surface morphology with triangular features having linear extents of  $\sim 60 \text{ nm}$  or less, while the surface particles tend to become elliptic after the addition of Li and Mg as exhibited in panels (b) and (c). Eventually in panel (d) the film exhibits a different dense morphology with elongated particles when the power increases to 80 W. A roughness of about few nanometers ( $\sim 6 \text{ nm}$ s) was determined for NiO:(Li, Mg) thin films with a tendency of a slight decrease with increasing Li Mg power.

### 3.3. Optical properties

In agreement with nonstoichiometric NiO films, the transmittance of the as deposited state is below 70%. With Li Mg power increasing, there is a significant decrease in optical absorbance associated with an increase in transmittance, especially in the blue range (Fig. 6 a–b). The average transmittance in the  $330 < \lambda < 500 \text{ nm}$  short wavelength is calculated to be 48%, 55%, 57% and 54% for Li Mg power 0 W, 10 W, 25 W and 80 W, respectively. The transmittance increases of 17% at 350 nm and the absorbance decreases of 23% at 320 nm from pure NiO to Ni Li Mg oxide (Li Mg power/25 W). The strong absorbance at  $\lambda < 320 \text{ nm}$  arises from the typical semiconductor bandgap, which is widened as a result of the Li Mg alloy power increase [4]. The absorbance edge of NiO:(Li, Mg) films is shifted to shorter wavelength and such blue shift arises from the substitution of Ni with Mg [24]. The calculated direct optical band gap increases from 3.81 eV for pure NiO films to 4.02 eV (Li Mg power/80 W) as summarized in inset of Fig. 6b. In addition, the reflectance increases before  $\lambda = 350 \text{ nm}$  and then decreases overall in the  $350 < \lambda < 800 \text{ nm}$  range but remains below 20% after Mg and Li additions.

Color properties of NiO:(Li, Mg) films were quantified using chromaticity coordinates (Table 3). La Commission Internationale de l'Eclairage (CIE), as the one commonly used color system, is based on color matching functions that are converted to tristimulus

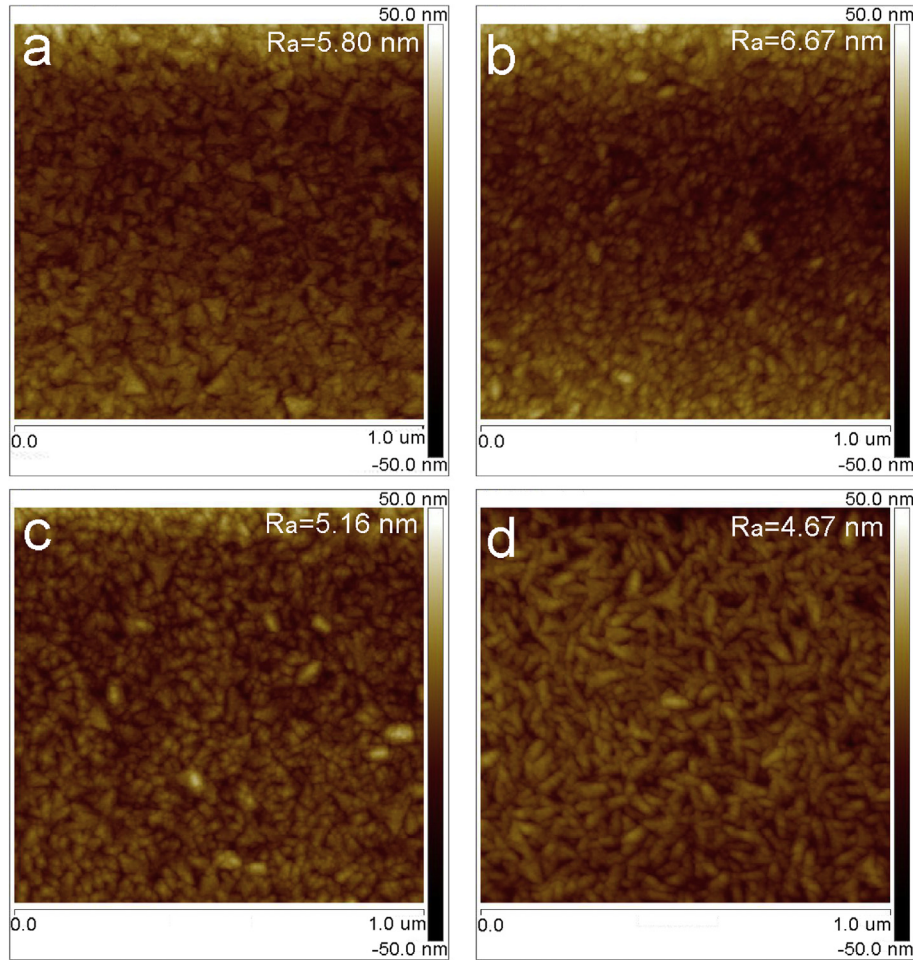


Fig. 5. The AFM micrographs for the pure NiO (a) and NiO:(Li, Mg) thin films for various Li-Mg powers (b) 10 W; (c) 25 W; (d) 80 W.

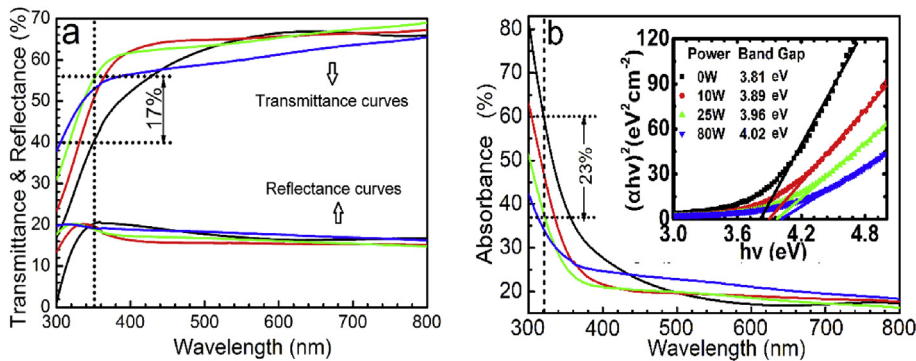


Fig. 6. (a) Transmittance and reflectance, (b) absorbance spectra of the NiO:(Li, Mg) thin films on quartz glass, Inset in panel (b) is plot of  $(\alpha hv)^2$  versus  $h\nu$ . (Black/red/green/blue curve corresponds to 0/10/25/80 W of Li-Mg power). (For interpretation of the references to color in this figure legend, the reader is referred to the Web version of this article.)

**Table 3**  
The chromaticity coordinates of NiO:(Li, Mg) films.

Li-Mg power	0	10	25	80
x-Red	0.3475	0.3385	0.3416	0.3422
y-Green	0.3501	0.3395	0.3411	0.3415
z-Blue	0.3024	0.3220	0.3173	0.3163

values [6]. The latter reflects the human perception of color and chromaticity coordinates (x, y, z) correspond to red, green and blue

primaries, respectively. Color neutrality is represented by (0.3333, 0.3333, 0.3333) [4]. Looking at the values for the 25 W, the z Blue component does increase from 0.3024 to 0.3173, closer to the desired 0.3333. It is evident that the additional guest elements changes the visual appearance towards a more color neutral state primarily by increasing the contribution of the blue part of the spectrum (i.e. the z component), which is consistent with the enhanced optical transmittance at 435 nm. Thereby, the color neutrality is improved, which corresponds to data in Table 3.

### 3.4. Electrochromic behavior

Electrochemical switching in Fig. 7 is carried out in non aqueous electrolyte (1 M PC/LiClO<sub>4</sub>, Pt counter electrode, Ag/AgCl reference), combined with *in situ* measurements of optical transmittance as shown in Fig. 8. For the 100th cycle, the CVs exhibit similar shapes and the reduction peaks (*I<sub>red</sub>*, *I<sub>red</sub>*) potentials appear close to that of the 2nd cycle while both oxidation peaks (*I<sub>ox</sub>*, *I<sub>ox</sub>*) shift towards a more positive potential compared to the 2nd cycle. Boschloo and Mihelcic [25,26] assumed that under oxidation the surface Ni<sup>2+</sup> ions are coupled with cation desorption (Li<sup>+</sup>), the nature of which determines the positions of the peaks. This leads them to conclude that the position and shape of peaks are not simply consistent with oxidation of Ni<sup>2+</sup> to Ni<sup>3+</sup> and Ni<sup>4+</sup>. In *in situ* optical transmittance measurement, only films with Li Mg power of 25 W exhibit an improvement in transparency of the bleached state as well as lower transmittance in colored state, which is to some degree related to different NiO morphologies as presented in AFM section. When Li Mg power increases to 25 W, film particles evolve from triangular to smaller uniform elliptic shapes, accompanied by more boundaries and increasing of specific surface areas. The boundaries provide more channels for the movements of ions and their reactivity within the films [27], which is closely related to the charge capacity. The charge capacity, together with electrochromic efficiency, will lead the optical transmittance. When the power increases to 80 W, however, a different dense morphology with elongated particles is accompanied by the decline of optical modulation. On the one hand, film morphology evolution can to some degree account for the excellent optical variation ability (25 W); on the other hand, the study of bleaching/coloration charge and high efficiency for 25 W (Fig. 9) also provides some evidence to support such optical behavior. A small Li Mg power (0 W, 10 W) could firstly decrease the film charge capacity while then there is an increase with power (25 W, 80 W). Particularly, the color efficiency, defined as the ratio of optical density to charge capacity, reaches its peak value when the power is 25 W in the 100th cycle. Overall, a better balance between bleaching and coloring charge/efficiency is achieved in the 100th cycle comparing to the 2nd cycle. Despite that the films show a decrease in charge capacity after 100 switching cycles (with the exception of power/10 W), the bleaching/coloration efficiency still shows a slight increase as compared to the initial cycle, which indicates films can evolve to better properties along with repeated electrochemical cycles. Summarizing, the advantage of incorporating Li and Mg elements (power/25 W) to NiO based films is obvious, which could not only bring enhanced optical transmittance in short wavelengths without compromising electrochemical properties, but bring long desired characteristics such as good cycling performance and excellent EC efficiency.

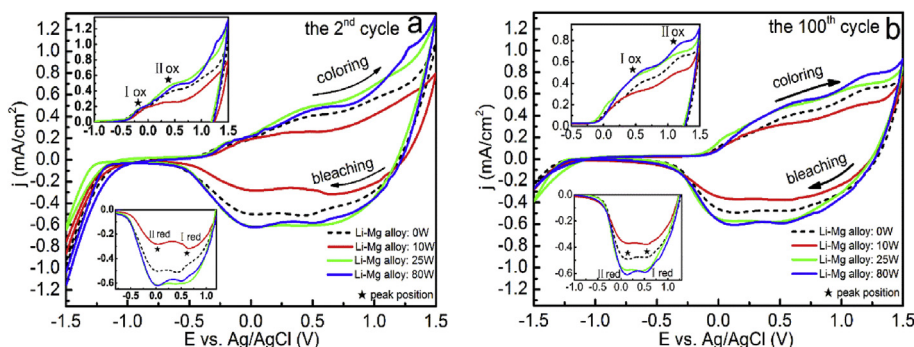


Fig. 7. (a) The 2nd and (b) 100th CVs of the NiO:(Li, Mg) films on ITO glass cycled in 1 M PC-LiClO<sub>4</sub> electrolyte with potential  $\pm 1.5$  V for different Li-Mg powers. Ag/AgCl was used as reference electrode and Pt as counter electrode. Scan rate: 0.1 V/s, active area:  $2.5 \times 3 \text{ cm}^2$ .

With regard to the NiO:(Li, Mg) films cycling in 1 M LiClO<sub>4</sub>/PC electrolyte, the EC efficiency value can reach as high as 60 cm<sup>2</sup>/C (Fig. 9) and response time for bleaching and coloration is 1.0 and 2.5 s, respectively (Fig. 10). The coloration efficiency value 40–60 cm<sup>2</sup>/C and switching time 1.3–3 s have been reported in the literature [28–30] for oxides, and in particular WO<sub>3</sub>. The comparable values directly prove that high transparency in short wave length is obtained without compromising the EC properties.

Typical variations of the bleached and colored transmittance spectra of NiO:(Li, Mg) oxide films as a function of Li Mg alloy power are shown in Fig. 10. The bleached transparency depicted in Fig. 11a is always higher than the initial (as deposited) state shown in Section 3.3, which confirms the existence of Ni<sup>3+</sup> ions [31] in NiO:(Li, Mg) films. The optical variations at 500 nm are 49%, 36%, 57% and 44% corresponding to 0 W, 10 W, 25 W and 80 W of Li Mg alloy power. It is noteworthy that in bleached states of the maximum transmittance, the optical modulation decreases with a small Li Mg power and then is significantly enhanced for the Mg Li containing film with power increasing to 25 W almost over the full spectra range. Again, the optical contrast shows a dramatic decline when the power is as large as 80 W. The most interesting is the flatness feature of the bleached state transmittance curve after a wavelength of 340 nm, as it is characteristic of a neutral color property. For the bleached films with different Li Mg powers, the difference in transmittance is especially large at  $330 < \lambda < 400 \text{ nm}$  and  $500 < \lambda < 600 \text{ nm}$  as shown in partial enlargement spectra in Fig. 11b. For the same Li Mg power 25 W, transmittance changes ( $\Delta T$ ,  $T_b$ ,  $T_c$ ) are obtained by performing *in situ* spectroelectrochemical measurements and presented as better colored states and enlarged  $\Delta T$  as a function of potential in Fig. 11c.  $\Delta T$  increases from 54 to 66% with potential ranging from  $\pm 1.5 \text{ V}$  to  $\pm 2 \text{ V}$ .

### 3.5. EC performance of NiO:(Li, Mg) based device

In light with an enhanced bleached transparency in short wavelengths (Fig. 6 a) and improved electrochemical charge capacity (Fig. 8) by NiO:(Li, Mg) 25 W films cycled in 1 M PC/LiClO<sub>4</sub> electrolyte, we fabricate inorganic all solid state unconventional lithium salt electrolyte (such as LiTaO<sub>3</sub>, LiNbO<sub>3</sub>, LiPON) free EC device: Glass/ITO/NiO:(Li, Mg)/Ta<sub>2</sub>O<sub>5</sub>/WO<sub>3</sub>/ITO. Li in NiO layer is the main factor contributing to the color change. Lithium free Ta<sub>2</sub>O<sub>5</sub> is applied as the electrolyte layer sharing two interfaces with the active materials in the device, assuring the color change of the complete device. The layers of the display are all prepared by sputtering and detailed deposition process can be found in our former work [32–34]. To the best of our knowledge, it is the first time that in the full EC device preparation economical commercial Li Mg alloy is used to incorporate Mg and Li elements to NiO films.

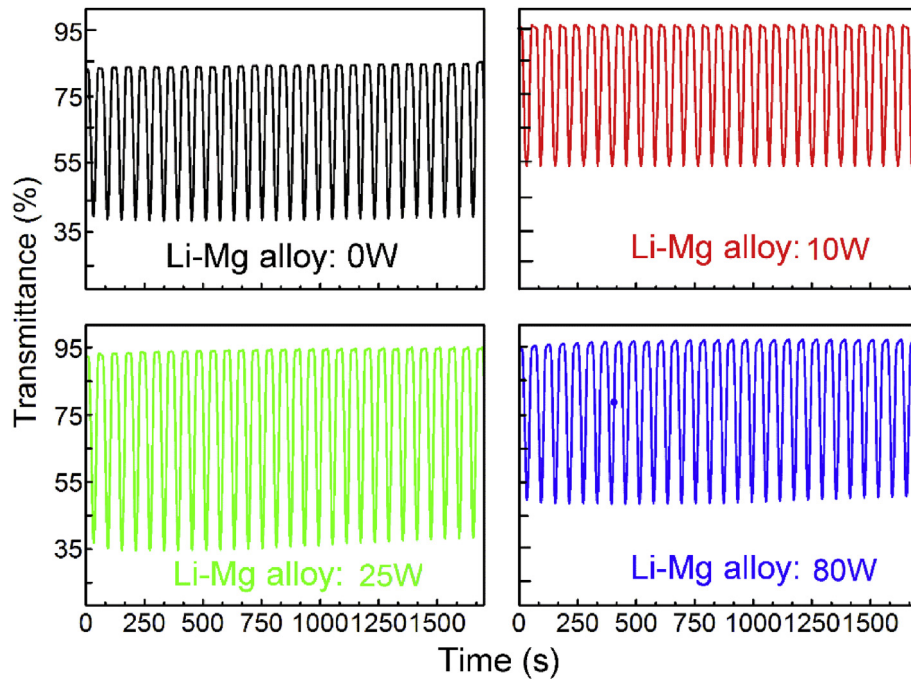


**Fig. 8.** *In situ* transmittance variation for the NiO:(Li, Mg) films at 550 nm cycled in 1 M PC- LiClO<sub>4</sub> electrolyte with potential  $\pm 1.5$  V. Ag/AgCl was used as reference electrode and Pt as counter electrode. Scan rate: 0.1 V/s. (Black/red/green/blue curve corresponds to 0/10/25/80 W of Li-Mg power). (For interpretation of the references to color in this figure legend, the reader is referred to the Web version of this article.)

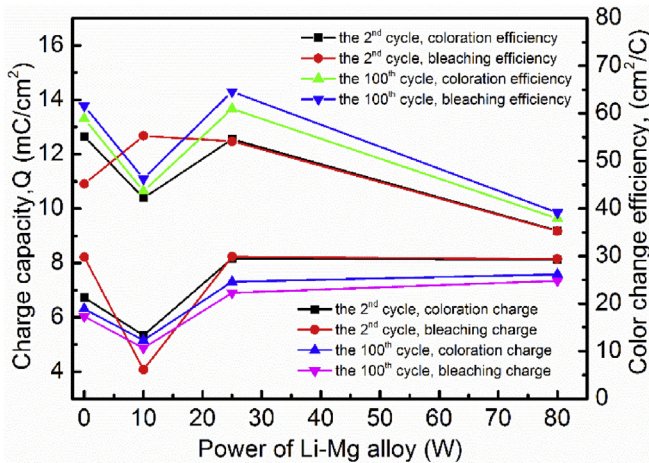


**Fig. 9.** Charge capacity and coloration efficiency of the NiO:(Li, Mg) films in 1 M LiClO<sub>4</sub>/PC electrolyte.

On one hand, Mg additive helps broaden optical gap and enhance bleached transparency in short wavelengths, meanwhile, improve electrochemical charge capacities. On the other hand, inorganic lithium driven device can be made successfully without applying LiTaO<sub>3</sub> or LiNbO<sub>3</sub> traditional ceramic targets [35].

As depicted in Fig. 12a, the EC modulation range enlarges with Li Mg power increasing from 0 to 25 W and then becomes smaller with power further increase to 80 W. When higher potential as well as longer bleaching/coloring time (100 s) is applied to the device (NiO:(Li, Mg) 25 W), higher transmittance variations can be achieved up to 56%. However, the device shows 4.5% optical modulation degradation when potential increases to 4.0 V (Fig. 12b). As a consequence, a voltage window of 3.5 V is applied to investigate the optical transmittance of the bleached/colored device in the full spectra (Fig. 12c). Here, the most interesting feature is the flatness of the transmittance curve after wavelength 400 nm, as it is characteristic of a neutral color property. Furthermore, the distinguished color neutrality of the full device is also evidenced by the chromaticity coordinates, with (0.3477, 0.3447, 0.3076) and

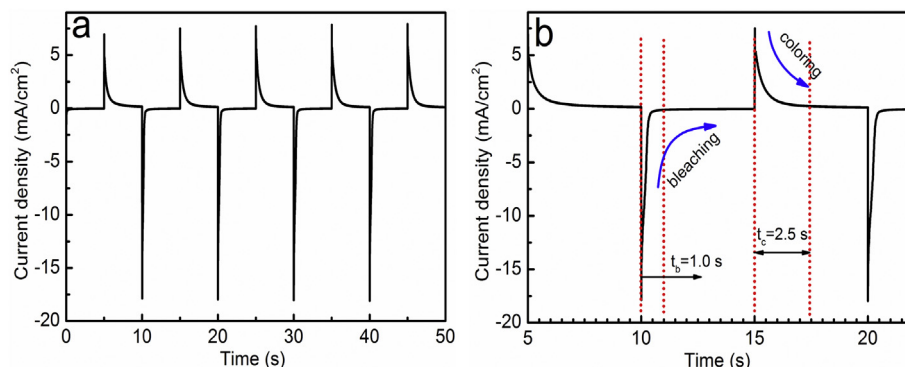


**Fig. 10.** Typical time response of the current density in the (a) 0–50 s and (b) 5–22 s time range of the NiO:(Li, Mg) films (25 W).

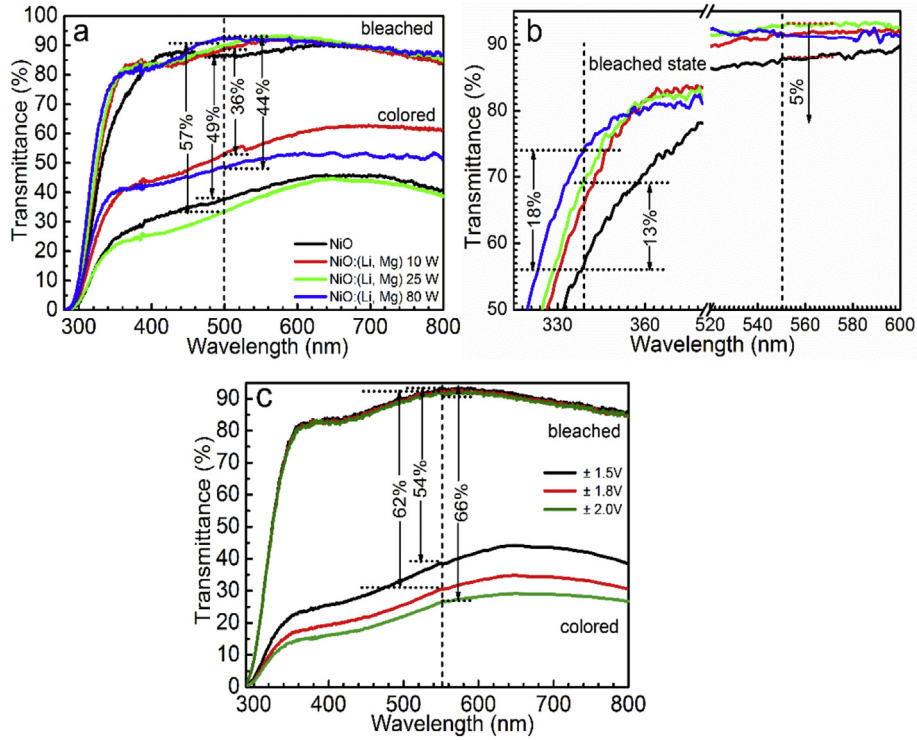


**Fig. 11.** (a) Transmittance curves, (b) partial enlargement for NiO:(Li, Mg) thin films at bleached and colored states with potential  $\pm 1.5$  V and (c) for different potentials windows ( $\pm 1.5$  V,  $\pm 1.8$  V,  $\pm 2.0$  V) for NiO(Li, Mg) 25 W.

(0.3395, 0.3312, 0.3293) of bleached and colored states, respectively. The neutrality of the full device is also confirmed by the calculation of the chromaticity parameters, with ( $a^*$ ,  $b^*$ ) values of

( 5, 3) in the colored state [36,37]. Additionally, the multiple layers can be clearly observed in the cross section of the device Glass/ITO/NiO:(Li, Mg)/Ta<sub>2</sub>O<sub>5</sub>/WO<sub>3</sub>/ITO (Fig. 12d).

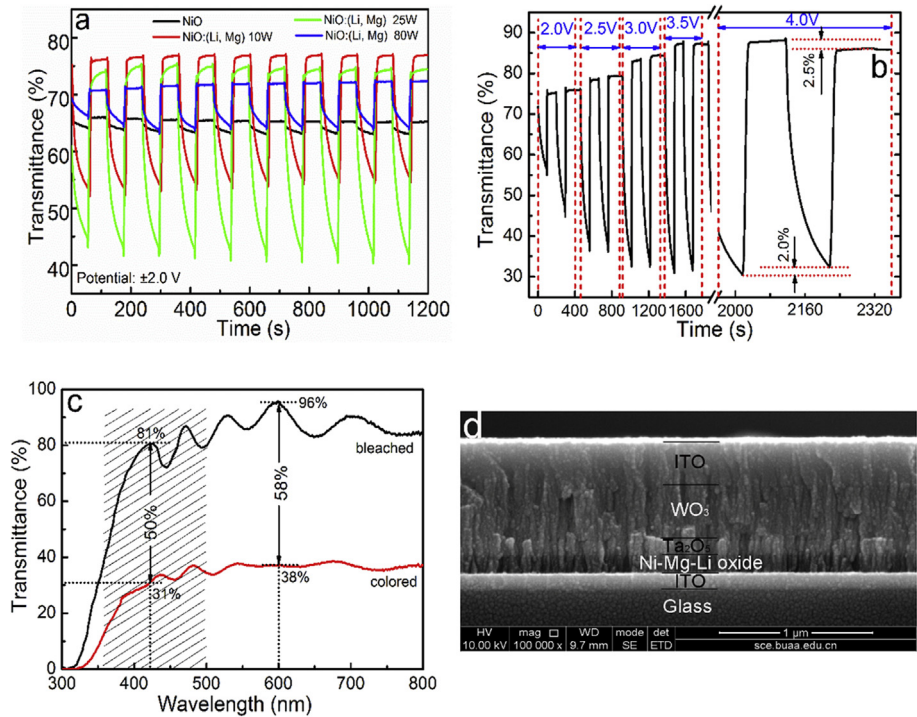


**Fig. 12.** (a) Multiple-cycle transmittance of the Glass/ITO/NiO:(Li, Mg)/Ta<sub>2</sub>O<sub>5</sub>/WO<sub>3</sub>/ITO EC device with various Li-Mg powers. The bleaching/coloring time is 60 s and the potential applied is  $\pm 2.0$  V. (b) Dynamic optical transmittance curve of EC device (NiO:(Li, Mg) 25 W) in function of operation potentials from  $\pm 2.0$  to  $\pm 4.0$  V at 550 nm. The bleaching/coloring time is 100s. (c) Optical transmittance curve in full spectra of EC device (NiO:(Li, Mg) 25 W) under operation potential  $\pm 3.5$  V and bleaching/coloring time as 100 s. (d) Cross-sectional image of a typical multilayered structure EC device.

## 4. Conclusion

For inorganic solid state EC devices that are driven by  $\text{Li}^+$  ions, until now, in most cases ceramic oxide targets are used for RF sputtering to realize the deposition of  $\text{LiTaO}_3$ ,  $\text{LiNbO}_3$  or  $\text{LiPON}$  inorganic electrolyte layer. A simplified method that can introduce  $\text{Li}^+$  ions into the device while avoiding ceramic oxide targets has been developed in our work by using Li containing alloy target. The co sputtering of Li Mg alloy and Ni targets is not only a good solution to introduce  $\text{Li}^+$ , but also can decrease the absorbance of NiO due to Mg doping. Comparing the chemical wet process method for introducing  $\text{Li}^+$ , the use of Li Mg alloy makes the device preparation simplified and more efficient. In our work, monolithic inorganic device Glass/ITO/NiO:(Li, Mg)/ $\text{Ta}_2\text{O}_5/\text{WO}_3/\text{ITO}$  with excellent electrochromic, EC, performance is successfully fabricated and the existence of Li as well as Mg within NiO based films is proved applying SIMS and XPS techniques. Using DC magnetron sputtering, the co doping of NiO with Mg and Li with the purpose of simultaneously widening the gap and avoiding the use of Li containing electrolyte, through NiO pre lithiation was investigated. Incorporation of Mg to NiO thin film is shown to broaden its optical band gap and enhance the bleached transparency in short wavelengths. NiO:(Li, Mg) films exhibit neutral color feature as well as good electrochemical cycling stability without sacrificing their charge capacities in particular for films grown using a Li Mg target with a power of 25 W. Li in NiO layer is the main factor contributing to the color change. In summary, on one hand, elements of Mg and Li can bring positive doping effect to Ni oxide. On the other hand, a different device without lithium salt electrolyte as the electrolyte layer can be fabricated. This new approach would benefit practical EC devices desired for their successful commercial applications and investigations are still ongoing.

## Acknowledgments

This work has been financially supported by the National Program on Key Research Project of China (2016YFB0303900), the Academic Excellence Foundation of BUAA for PhD Students (2017062), the Beijing Natural Science Foundation (2161001) and the Fundamental Research Funds for the Central Universities (Grant No. YWF 16 JCTD B 03).

Authors acknowledge T. Hungria from UMS Castaing, Université de Toulouse for providing the SIMS characterization of the device.

## References

- [1] R. Kotz, C. Barbeo, O. Haas, Probe beam deflection investigation of the charge storage reaction in anodic iridium and tungsten oxide films, *J. Electroanal. Chem. Interfacial Electrochem.* 296 (1990) 37–49.
- [2] R. Kotz, H. Neff, Anodic iridium oxide films: an UPS study of emersed electrodes, *Surf. Sci.* 160 (1985) 517–530.
- [3] A. Azens, G. Vaivars, M. Veszelei, L. Kullman, C.G. Granqvist, Electrochromic devices embodying W oxide/Ni oxide tandem films, *J. Appl. Phys.* 89 (2001) 7885–7887.
- [4] A. Azens, J. Isidorsson, R. Karmhag, C.G. Granqvist, Highly transparent Ni Mg and Ni V Mg oxide films for electrochromic applications, *Thin Solid Films* 422 (2002) 1–3.
- [5] A. Azens, C.G. Granqvist, Electrochromism in Ir Mg oxide films, *Appl. Phys. Lett.* 81 (2002) 928–929.
- [6] E. Avendano, A. Azens, G.A. Niklasson, C.G. Granqvist, Electrochromism in nickel oxide films containing Mg, Al, Si, V, Zr, Nb, Ag, or Ta, *Sol. Energy Mater. Sol. Cell.* 84 (2004) 337.
- [7] Y. Chen, O. Sakata, R. Yamauchi, A. Yang, L.S.R. Kumara, C. Song, N. Palina, M. Taguchi, T. Ina, Y. Katsuya, H. Daimon, A. Matsuda, M. Yoshimoto, Lattice distortion and electronic structure of magnesium-doped nickel oxide epitaxial thin films, *Phys. Rev. B* 95 (2017) 245301–245311.
- [8] C. Arbizzani, M.G. Ceroni, M. Mastragostino, Polymer-based symmetric electrochromic devices, *Sol. Energy Mater. Sol. Cell.* 56 (1999) 205–211.
- [9] X.P. Zhang, H.K. Zhang, Q. Li, H.L. Luo, An all-solid-state inorganic electrochromic display of  $\text{WO}_3$  and NiO films with  $\text{LiNbO}_3$  ion conductor, *IEEE Electron. Device Lett.* 21 (2000) 215–217.
- [10] L. Su, Q. Hong, Z. Lu, Structural and luminescent properties of  $\text{Eu}^{3+}$  doped  $\text{Gd}_{17.33}(\text{BO}_3)_4(\text{B}_2\text{O}_5)_2\text{O}_{16}$ , *J. Mater. Chem.* 8 (1998) 1051–1054.
- [11] S. Oukassi, C. Giroud-Garampon, C. Dubarry, C. Ducros, R. Salot, All inorganic thin film electrochromic device using LiPON as the ion conductor, *Sol. Energy Mater. Sol. Cell.* 145 (2016) 2–7.
- [12] Q. Liu, G.B. Dong, Y. Xiao, F.Y. Gao, M. Wang, Q. Wang, S. Wang, H.P. Zuo, X.G. Diao, An all-thin-film inorganic electrochromic device monolithically fabricated on flexible PET/ITO substrate by magnetron sputtering, *Mater. Lett.* 142 (2015) 232–234.
- [13] B. Kasel, T. Wirtz, Si useful yields measured n Si, SiC,  $\text{Si}_3\text{N}_4$  and  $\text{SiO}_2$ : comparison between the storing matter techniques and SIMS, *Surf. Interface Anal.* 46 (2014) 39–42.
- [14] H. Seyama, M. Soma, X-ray photoelectron spectroscopic study of montmorillonite containing exchangeable divalent cations, *J. Chem. Soc. Faraday Trans. 80* (1984) 237–248.
- [15] R. Jerome, Ph Theyssie, J.J. Pireaux, J.J. Verbist, Surface analysis of polymers end-capped with metal carboxylates using X-ray photoelectron spectroscopy, *Appl. Surf. Sci.* 27 (1986) 93–105.
- [16] J.P. Contour, A. Salesse, M. Froment, M. Garreau, J. Thevenin, DJ. Warin *Microsc. Spectrosc. Electron.* 4 (1979) 483.
- [17] Y.Y. Tian, W.K. Zhang, S. Cong, Y.C. Zheng, F. Geng, Z.G. Zhao, Unconventional aluminum ion intercalation/deintercalation for fast switching and highly stable electrochromism, *Adv. Funct. Mater.* 25 (2015) 5833–5839.
- [18] R.D. Shannon, Revised effective ionic radii and systematic studies of interatomic distances in halides and chalcogenides, *Acta Crystallogr.* 32 (1976) 751–767.
- [19] M. Wang, Y. Thimont, L. Presmanes, X. Diao, A. Barnabé, The effect of the oxygen ratio control of DC reactive magnetron sputtering on as-deposited non stoichiometric NiO thin films, *Appl. Surf. Sci.* 419 (2017) 795–801.
- [20] T.K. Bechgaard, G. Scannellb, L. Huangb, R.E. Youngmanc, J.C. Mauroc, M.M. Smedskjaer, Structure of MgO/CaO sodium aluminosilicate glasses: Raman spectroscopy study, *J. Non-Cryst. Solids* 470 (2017) 145–151.
- [21] Y. Kowada, H. Adachi, M. Tatsumisagu, T. Minami, High temperature Raman spectra of  $\text{Li}_2\text{O}-\text{P}_2\text{O}_5$  melts with large amounts of  $\text{Li}_2\text{O}$ , *Nippon Seramikkusu Kyokai Gakujutsu Ronbunshi* 98 (1990) 108–109.
- [22] C. Julien, M. Massot, Raman scattering of  $\text{LiNi}_{1-y}\text{Al}_y\text{O}_2$ , *Solid State Ionics* 148 (2002) 53–59.
- [23] P.S. Mahadik, P. Sengupta, R. Halder, G. Abraham, G.K. Dey, Perovskite Ni composite: a potential route for management of radioactive metallic waste, *J. Hazard Mater.* 287 (2015) 207–216.
- [24] M. Ben Amor, A. Boukhachem, K. Boubaker, M. Amlouk, Structural, optical and electrical studies on Mg-doped NiO thin films for sensitivity applications, *Mater. Sci. Semicond. Process.* 27 (2014) 994.
- [25] G. Boschloo, A. Hagfeldt, Electrochemical investigation of traps in a nanostructured  $\text{TiO}_2$  film, *J. Phys. Chem. B* 105 (2001) 3039.
- [26] M. Mihelcic, A. Surca Vuk, I. Jerman, B. Orel, F. Švegl, H. Moulki, C. Faure, G. Campet, A. Rougier, Comparison of electrochromic properties of  $\text{Ni}_{1-x}\text{O}$  in lithium and lithium-free aprotic electrolytes: from  $\text{Ni}_{1-x}\text{O}$  pigment coatings to flexible electrochromic devices, *Sol. Energy Mater. Sol. Cell.* 120 (2014) 116.
- [27] S.R. Jiang, P.X. Yan, B.X. Feng, X.M. Cai, J. Wang, The response of a NiOx thin film to a step potential and its electrochromic mechanism, *Mater. Chem. Phys.* 77 (2002) 384–389.
- [28] G. Zukowska, E. Zygadlo-Monikowska, N. Langwald, Z. Florjanczyk, R. Borkowska, P. Kuzma, W. Wiczorek, S. Greenbaum, S.H. Chung, Proton-conducting polymer gels as new materials for electrochemical applications, *J. New Mater. Electrochem. Syst.* 3 (2000) 241–247.
- [29] M. Hepel, H. Redmond, I. Dela, Electrochromic  $\text{WO}_3_x$  films with reduced lattice deformation stress and fast response time, *Electrochim. Acta* 52 (2007) 3541–3549.
- [30] M. Hepel, L.I. Dela-Moss, H. Redmond, Lattice polarization effects in electrochromic switching in  $\text{WO}_3-x$  films studied by pulse-nanogravimetric technique, *J. Solid State Electrochem.* 18 (2014) 1251–1260.
- [31] J. Jensen, M. Hosel, A.L. Dyer, F.C. Krebs, Development and manufacture of polymer-based electrochromic devices, *Adv. Funct. Mater.* 25 (2015) 2073.
- [32] D.M. Dong, W.W. Wang, G.B. Dong, Y.L. Zhou, Z.H. Wu, M. Wang, F.M. Liu, X.G. Diao, Electrochromic properties of  $\text{NiO}_x:\text{H}$  films deposited by DC magnetron sputtering for ITO/ $\text{NiO}_x:\text{H}/\text{ZrO}_2/\text{WO}_3/\text{ITO}$  device, *Appl. Surf. Sci.* 357 (2015) 799–805.
- [33] D.M. Dong, W.W. Wang, G.B. Dong, Y.L. Zhou, Z.H. Wu, M. Wang, F.M. Liu, X.G. Diao, Electrochromic properties and performance of  $\text{NiO}_x$  films and their corresponding all-thin-film flexible devices prepared by reactive DC magnetron sputtering, *Appl. Surf. Sci.* 383 (2016) 49–56.
- [34] D.M. Dong, W.W. Wang, G.B. Dong, F. Zhang, H. Yu, Y.C. He, X.G. Diao, Improved performance of Co-sputtered Ni Ti oxide films for all-solid-state electrochromic devices, *RSC Adv.* 6 (2016) 111148–111160.
- [35] J. Gou, J. Wang, M. Yang, Z. Huang, W. Li, Y. Jiang, Preparation and characterization of  $\text{LiTaO}_3$  films derived by an improved sol-gel process, *Acta Metall. Sin.* 26 (2013) 299–302.
- [36] H. Moulki, D.H. Park, B.K. Min, H.S. Kwon, S.J. Hwang, J.H. Choy, T. Toupance, G. Campet, A. Rougier, Improved electrochromic performances of NiO based thin films by lithium addition: from single layers to devices, *Electrochim. Acta* 74 (2012) 46–52.
- [37] [www.efg2.com/Lab/Graphics/Colors/Chromaticity.htm/2012](http://www.efg2.com/Lab/Graphics/Colors/Chromaticity.htm/2012).